Dissipation Processes at the Mesoscopic and Molecular Scale. The Case of Polymer Films

M.Voué,[‡] M. P. Valignat,[†] G. Oshanin,[§] and A. M. Cazabat*,[†]

Collège de France, Physique de la Matière condensée 11, place Marcelin Berthelot, 75231 Paris Cédex 05, France, Université de Mons-Hainaut, Modélisation Moléculaire, 20 place du Parc, 7000 Mons, Belgium, and Université Paris VI, Physique Théorique des Liquides 4, place Jussieu, 75252 Paris Cedex 05, France

Received May 11, 1998. In Final Form: November 4, 1998

The spontaneous spreading of liquid films results from the balance between an energetic driving term and dissipative processes. For films of mesoscopic thickness, the dissipative term is proportional to the bulk viscosity η of the liquid. For thinner films, the observed dynamics depends also on the friction coefficient ζ_1 of the first molecular layer of liquid on the solid. For high friction, the overall film growth should be mainly controlled by the value of η. For low friction, the friction coefficient ζ_1 should become the leading parameter. This behavior is investigated in the framework of the model of a stratified droplet recently proposed by de Gennes. Complementary information is provided by numerical simulations when solid−liquid interactions (which control the value of ζ_1) are modified keeping the liquid−liquid ones the same (i.e., the bulk viscosity η). Moreover, the numerical simulations provide information on molecules displacements inside the droplet. Experiments were performed with short polymer chains below the three-dimensional disentanglement threshold, where the polymer behaves as a simple, nonvolatile liquid. High and low friction correspond to different thickness profiles. The dynamics of the first layer in both cases agrees with the theoretical expectations.

Introduction

The spreading dynamics of nonvolatile liquids, and more specifically the relation between the liquid velocity and the dynamic contact angle, has been investigated for long, both theoretically and experimentally.[1−12] Basically, the spreading results from the balance between energetic driving terms and dissipative processes. Various theories have been proposed, differing mainly in the way dissipation is treated. Hydrodynamical approaches[1−10] put emphasis on the role of the bulk viscosity η, while the molecular theory[11,12] focuses on the dissipation at the contact line. Recent progress has been done for developing an unified theory, where both viscosity and dissipation at the contact line are considered.[12,13]

The present study addresses a similar problem, but now in the molecular range of thickness and in the complete wetting case. The bulk parameter for dissipation is again the viscosity η, and the molecular parameter is the friction coefficient ζ_1 of the first molecular layer of liquid on the solid.

We shall organize the discussion in the framework of the stratified droplet model proposed by de Gennes, because the viscosity and the friction coefficient ζ_1 explicitely appear in the equations.[14] This model allows one to understand how the drop shape is controlled by the relative weight of the two dissipative processes. However, only trends can be obtained for the spreading dynamics. In the second part of the paper, these results will be compared with computer simulations, and in the last part with experiments. The trick used to make the difference between η and ζ_1 in experiments is to use polymers in the crossover between the short chain behavior below the entanglement threshold (η proportional to the molar mass M) and the long chain behavior above (η proportional to $M^{3.4}$). Since η and ζ_1 display different dependence on M, we are able to single out the leading dissipation channel.

The Stratified Droplet Model

This model has been extensively presented and discussed elsewhere.[14−15]

For the problem considered here, we just recall that the liquid is incompressible, nonvolatile, and wets the substrate completely. The droplet has a constant volume and is assumed to be completely stratified in layers of thickness a.

The friction coefficients $\zeta_{n,n-1}$ between successive liquid layers are for simplicity assumed to have the same value ζ, while the friction coefficient between the first layer and the surface is ζ_1. Note that if the area per molecule in a layer is Σ, the bulk viscosity is

[†] Collège de France.

[‡] Université de Mons-Hainaut.

[§] Université Paris VI.

(1) Fairbrother, F.; Stubbs, A. *J. Chem. Soc.* **1935**, *1*, 527. Bretherton, F. P. *J. Fluid Mech.* **1961**, *10*, 166.
(2) Huh, C.; Scriven, L. E. *J. Colloid Interface Sci.* **1971**, *35*, 85.
(3) Voinov, O. V. *Fluids Dyn.* **1976**, *11*, 76.
(4) Derjaguin, B. V.; Churaev, N. V. *Wetting Films*; Nauka, Moscow, 1984; Derjaguin, B. V.; Churaev, N. V.; Muller, V. M. *Surface forces*; Consultant Bureau: New York, 1987. Churaev, N. V. *Rev. Phys. Appl.* **1988**, *23*, 975.
(5) Dussan V, E. B. *Annu. Rev.Fluid Mech.* **1979**, *11*, 371. Dussan V, E. B.; Davis, S. J. *Fluid Mech.* **1974**, *65*, 71.
(6) Tanner, L. H. *J. Phys. D* **1979**, *12*, 1478.
(7) Hoffmann, R. L. *J. of Colloid Interface Sci.* **1983**, *94*, 470.
(8) Starov, V. M. *Kolloidn. Zh.* **1983**, *45*, 1154.
(9) e Gennes, P. G. *Rev. Mod. Phys.* **1985**, *57*, 827.
(10) Cox, R. G. *J. Fluid Mech.* **1986**, *168*, 169.
(11) Blake, T. D. How do wetting lines move? Presented at the AIChE Spring Meeting, New Orleans, LA, 1988 (Paper 1a). Cherry, B. W.; Holmes, C. M. *J. Colloid Interface Sci.* **1969**, *29*, 174.
(12) Blake, T. D. Dynamic contact angles and wetting kinetics. In Wettability; Berg, J. C., Ed.; Surfactant Science Series 49; Marcel Dekker: NY, 1993; p 251.
(13) de Ruijter, M.; De Coninck, J.; Oshanin, G. *Langmuir* 1998. Manuscript to be published.
(14) de Gennes, P. G.; Cazabat, A. M. *C. R. Seances Acad. Sci. Sér. 2*, **1990**, *310*, 1601.
(15) Fraysse, N.; Valignat, M. P.; Cazabat, A. M.; Heslot, F.; Levinson, P. *J. Colloid Interface Sci.* **1993**, *158*, 27.

10.1021/la9805600 CCC: $18.00
Published on Web 01/14/1999

$$\eta = \frac{a\zeta}{\Sigma} \tag{1}$$

Therefore, ζ and η are equivalent parameters.

The dynamical equations for the radii R_1 and R_2 of the first and second layer are

$$R_1\frac{dR_1}{dt} = \frac{W_2 - W_1}{\zeta_1 \ln\frac{R_1}{R_2}} \tag{2}$$

$$R_1\frac{dR_1}{dt} + R_2\frac{dR_2}{dt} = \frac{W_3 - W_2}{\zeta \ln\frac{R_2}{R_3}}\left[1 + 4\frac{\zeta}{\zeta_1}\right] \tag{3}$$

Here, the W_n are the energies of the molecules in the nth layer. More generally, one may write

$$R_1\frac{dR_1}{dt} + ... + R_n\frac{dR_n}{dt} = \frac{W_{n+1} - W_n}{\zeta \ln\frac{R_n}{R_{n+1}}}\left[A_n + B_n\frac{\zeta}{\zeta_1}\right] = Q_n \tag{4}$$

where the parameters A_n and B_n are given by

$$A_n = \frac{n(n+1)(2n+1)}{6} - n^2 \qquad B_n = n^2 \tag{5}$$

For the dynamics of the successive radii, one has

$$R_n\frac{dR_n}{dt} = Q_n - Q_{n-1} \tag{6}$$

Mathematically speaking, the conclusion is that, for $\zeta \gg \zeta_1$, the dissipation is controlled by ζ_1 and conversely for $\zeta \ll \zeta_1$, by ζ. For a finite, given value of ζ/ζ_1, as A_n/B_n increases with increasing n, ζ_1 is the control parameter at low n, and ζ at large n (i.e., in the mesoscopic part of the drop).

Except for these trends, one has to be very careful when using the stratified droplet model in a predictive way, because the range of ζ/ζ_1 belonging to the domain of validity of the model is relatively ill-defined:

At low ζ/ζ_1 ($\zeta/\zeta_1 \ll 1$), the first layer is practically static. In the reality, spreading will mainly proceed through the "caterpillar" process proposed by Dussan,[5] the only dissipation being actually the viscous one. The molecules of the second layer reach the edge of the first layer, go onto the surface where they are trapped, and become part of this almost static first layer. The radii of the two first layers are equal and increase with time. However, this process is forbidden by the mere structure of the stratified droplet model, where the ratios R_n/R_{n+1} of successive radii have to be larger than 1 (see eqs 2−4). The molecules of the second layer cannot reach the surface if the first layer is static. The spreading just stops.

At large ζ/ζ_1 ($\zeta/\zeta_1 \gg 1$), the drop profile becomes very steep.[15] This profile is ultimately not compatible with the assumptions of the stratified droplet model, where the difference between successive radii has to be much larger than the permeation length.

One must be aware that in both cases, the model will still give plausible results, which means that we have no precise way to determine the range of ζ/ζ_1 allowed around the central value 1. This point will be further discussed in the following.

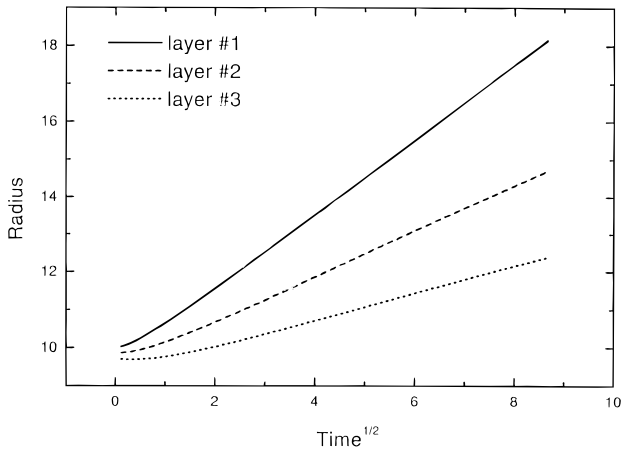

Figure 1. Growth of the radii of the three first layers as a function of the square-root of the time. The parameter of the stratified drop was $k = \zeta/\zeta_1 = 0.5$ with ζ=1.0 and $\zeta_1 = 2.0$. After some time, the radii grow linearly with $t^{1/2}$.

In the mesoscopic range of thickness (i.e., large n), the bulk viscosity will always become the relevant parameter for dissipation. This agrees with hydrodynamical theories[1−10] and also with the unified theory referred to above,[13] because our times scales correspond to the "long time behavior" of that theory, where dissipation is actually controlled by bulk viscosity. One might try to make a mathematical connection between the stratified droplet model and the study of mesoscopic spreading films developed by de Gennes and Joanny[16] in a one-dimensional geometry. This is, however, not straightforward because the stratified droplet model explicitely contains the conservation of drop volume.

Being now aware of the trends and limitations of the model, let us discuss further the time dependence of the successive radii in the case where $\zeta/\zeta_1 \approx 1$.

The presence of the logarithms in the formulas indicates that the process is not governed by true diffusive-like equations. On the other hand, experiment shows that the sucessive radii grow with the square root of time over the main part of the drop spreading process. This cannot be explained by the mere fact that a logarithm "is known to vary slowly". Here, at least for $n > 1$, the ratios of the radii are close to 1, and therefore the logarithms are roughly proportional to the differences $R_n - R_{n+1}$. Even if the right-hand side in the differential equations would be a constant, this would mean R^2 to be linear in t, not R to be linear in $t^{1/2}$, which would be true only when the initial radius has become negligible.

A numerical integration of the coupled differential equations may be carried out using a standard fourth-order Runge−Kutta method and an adaptative algorithm for the integration time step.[17] The drop is composed of 30 layers. The interactions are assumed to be given by van der Waals formula, $W_n = K/n^3$, and the initial drop shape is a truncated spherical cap.

The three first radii have been plotted as a function of the square root of time on Figure 1 for $\zeta/\zeta_1 = k = 0.5$, and for $k = 1.18$ on Figure 2. The plots are linear, in good agreement with experiments. This is not a trivial result which could be easily obtained considering the mathematical structure of the equations and the fact that the radii do not exceed greatly the initial ones.

(16) Joanny, J. F.; e Gennes, P. G. *J. Phys. Paris* **1986**, *47*, 121.
(17) Press, W. H.; Teukolsky, S. A.; Vetterlink, W. T.; Flannery, B. P. *Numerical Recipes in FORTRAN: The Art of Scientific Computing*, Cambridge University Press: Cambridge, 1992.

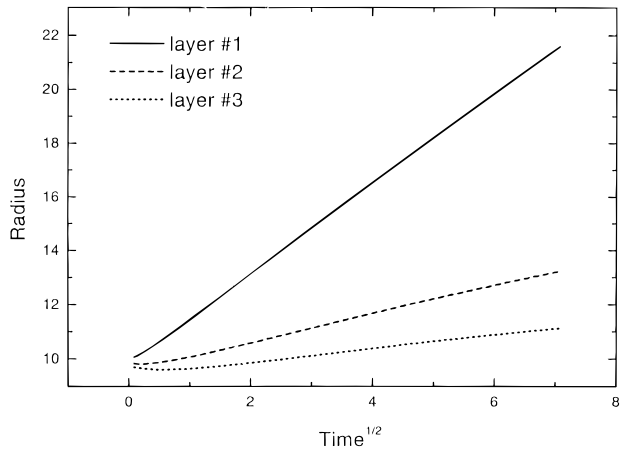

Figure 2. Dynamics of the radii for $k = 1.18$ ($\zeta = 1.0$ and $\zeta_1 = 0.85$).

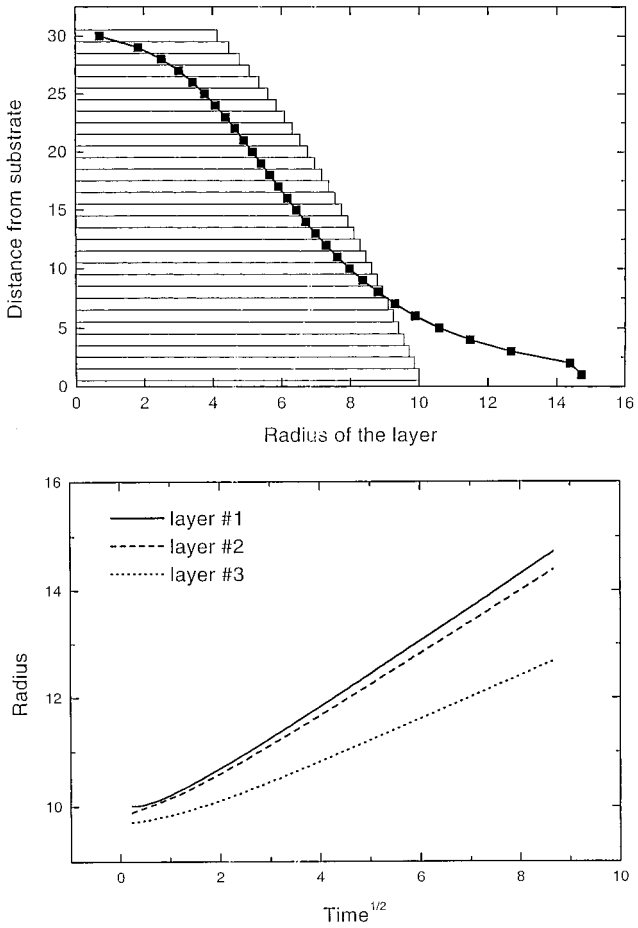

Figure 3. (a) Drop profile calculated for $k = 0.12$. The horizontal bars represent the initial profile. The line corresponds to the drop profile at $t = 75$. For this low value of k (i.e., for large values of ζ_1), the profile is smooth and the layers 1 and 2 have almost the same radius. (b) Dynamics of the radii showing that the two first layers are growing almost at the same rate.

Next, we have tried to use this numerical resolution to illustrate the role of k on the shape of the drop and on the spreading dynamics, for $0.1 \leq k \leq 10$, although we do not know if the model is valid over that whole range of k.

Let us first discuss the drop shape: Figure 3 corresponds to $k = 0.12$. All the layers grow more or less at the same rate. Figure 4 illustrates the opposite case $k = 10$. Only the first layer grows. The profile of the drop becomes quite steep. This corresponds to the fact that the flow in the first layer is large because of the low value of ζ_1, and that

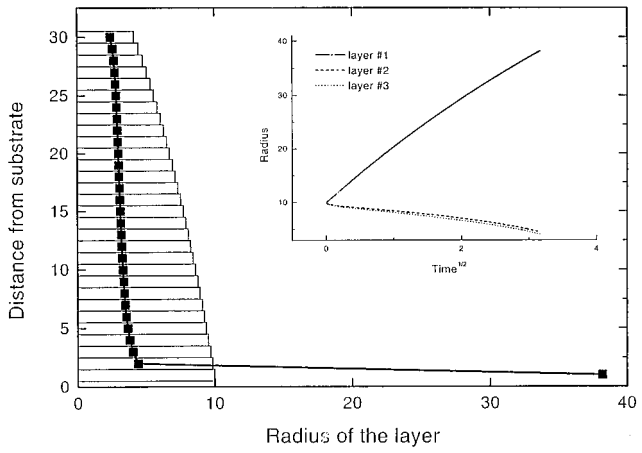

Figure 4. Drop profile calculated at low surface friction ($k = 10.0$) at $t = 10$: only the first layer grows in front of the mesoscopic part of the drop. Except for that layer, the profile is very steep. Comparison with the initial profile of the drop (horizontal bars) shows that all the subsequent layers are receding. Inset: Dynamics of the layers showing the rapid increase of the first one and the retraction of the others at the same rate. At long times, the curve R_1 vs $t^{1/2}$ deviates somewhat from linearity.

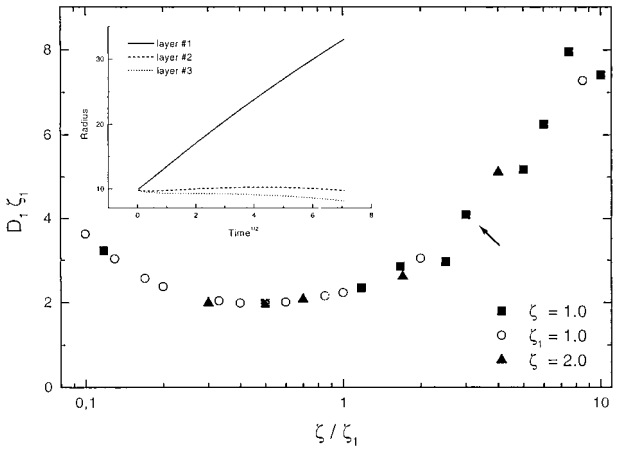

Figure 5. Variations of $D_1\zeta_1$ as a function of ζ/ζ_1. Inset: Dynamics of the layers for $k = 3.0$, indicating that the increase in $D_1\zeta_1$ at $k \geq 2$ occurs when the second layer starts to recede (i.e., when all layers recede except the first one).

this flow comes from the next upper layer, and so on. For the layers above the first one, the way to provide a large flow is to reduce the logarithmic term, which means that the radii become close[18] (i.e., the profile becomes steep).

Results on the dynamics of the first layer, as obtained by the numerical resolution, are summarized in Figure 5. Let us define the "diffusion coefficient" D_1 of the first layer through the slope of the curve, i.e.,

$$\frac{dR_1(t)}{d(\sqrt{t})} \approx \sqrt{D_1} \approx \text{cst} \qquad (7)$$

In the figure, we have plotted $\zeta_1 D_1$ as a function of $\zeta/\zeta_1 = k$. A single curve is obtained (i.e., in the range of time investigated $\zeta_1 D_1$ depends on ζ and ζ_1 only through their ratio k). The product $\zeta_1 D_1$ goes through a flat minimum between $k = 0.2$ and $k = 2$. In this range, D_1 scales such as $1/\zeta_1$.

(18) Villette, S.; Valignat, M. P.; Cazabat, A. M.; Jullien, L.; Tiberg, F. *Langmuir* **1996**, *12*, 825.

At lower k, the viscosity comes into play, which is satisfactory. For the lowest k values, one may approach the limit of validity of the model, as suggested by the change of concavity at the edge of the drop profile, visible on Figure 3. This may indicate that the flow pattern in the droplet will ultimately become caterpillar-like.

At larger k, the increase in $\zeta_1 D_1$ is probably nonphysical: the model does not contain dissipation in the case of a quasi vertical flow. The values $k \geq 3$ correspond to the case where all the layers recede except the first one (see inset Figure 5), a situation which we never met experimentally at short times: which is always observed is that the profile above the first layer is quasi vertical but widens slowly.

The conclusion of this numerical study is that the information on drop shape evolution with k is clear. The square root of time law is satisfactorily accounted for. However, only trends are obtained for the values of "diffusion coefficients", because the model might well be valid only in the reduced range $0.1 \leq k \leq 2$.

Complementary information on the drop profiles and dynamics can be obtained through computer simulations. Viscosity and friction coefficient can be modified independently. The strength of liquid−liquid interaction controls the viscosity, while changing the liquid−solid ones plays on the friction parameter ζ_1. Let us briefly present the results.

Computer Simulations

Monte Carlo techniques[19] and Molecular dynamics (MD) simulations[20−24] are widely used in the field of wetting and spreading. The model used in the present study has been extensively described in previous publications[20,23−24] and will be only briefly outlined. The basic interactions considered are of Lennard-Jones type

$$V_{ij}(r) = \frac{C_{ij}}{r^{12}} - \frac{D_{ij}}{r^6} = 4\epsilon_{ij}\left[\left(\frac{\sigma}{r}\right)^{12} - \left(\frac{\sigma}{r}\right)^{6}\right] \qquad (8)$$

where r denotes the interatomic distance. The parameters C_{ij} and D_{ij} refer to the fluid/fluid (ff), fluid/solid (fs), and solid/solid (ss) interactions and are related to the standard energy ϵ_{ij} and diameter σ of the LJ potential. These interactions are cut off when the interatomic distance is larger than $r_c = 2.5\,\sigma$. For simplicity, we chose $C_{ff} = D_{ff} = 1$ and $C_{fs} = D_{fs}$.

The atoms of the fluid are aggregated into 16-atom chain molecules by adding a intramolecular confining potential which, for computational convenience, scales as r^{-6}. The solid substrate is one layer of fcc lattice with the (100) surface in contact with the fluid. The solid atoms vibrate around an equilibrium position. Their velocities are rescaled in such a way that the temperature of the substrate is kept constant. This allows us to mimic the dry spreading experiments of the silicon oils that are described in the next part of the paper. Typically, 25 000 atoms and 300 000 atoms are considered for the liquid molecules and the solid, respectively.

Given all the inter- and intramolecular interaction potentials, the Newton's equation of motion are integrated using a predictor-corrector method. The integration time step $\Delta\tau$ is $5 \times 10^{-3}\,\tau$, where τ is the reduced time unit defined by $\tau = (\epsilon/m\sigma^2)^{1/2}$, m being the mass of the atoms of the liquid.

With that model, both partial wetting[23] and complete wetting[20,24] regimes can be described by varying the intensity of the solid/fluid coupling parameters $C_{fs} = D_{fs}$. For values of these parameters larger than approximately 0.8, a complete spreading of the liquid droplet is observed.

Contrarily to the experimental systems, the liquid−liquid interactions can be kept constant in the MD technique, independently of the liquid−solid coupling. Thus our simulations make possible to probe the direct influence of the substrate surface energy on the spreading process. But varying the C_{fs} and D_{fs} parameters is equivalent to modifying both the driving term and the friction, making their cumulative effects on the spreading rate quite complicated.

In a recent article,[24] we showed that the diffusion coefficient D_1 of the first layer goes through a maximum when the solid/liquid interaction is increased. The maximum is reached for $C_{fs} = D_{fs} \approx 1.2$ (i.e., for substrates of intermediate surface energies). Increasing the parameters from $C_{fs} = D_{fs} = 0.8$ to 1.2 increases the driving term more than the friction one and accelerates the spreading process.[24] Conversely, increasing C_{fs} and D_{fs} above the critical value 1.2 mainly increases the friction of the liquid molecules on the solid substrate, and the spreading slows down.

In the stratified droplet model the driving term does not change when friction parameters are modified. As a result, the "weak friction" regime (i.e., fast spreading) obtained for high values of k (low values of ζ_1) corresponds in MD to values of C_{fs} and D_{fs} close to 1.2. Conversely, low k values correspond to C_{fs} and D_{fs} larger than 1.2. Note that we are only comparing trends, not the profiles themselves: the stratified droplet model includes long range interaction, which is not the case for numerical simulations. Moreover, the results are not strictly comparable: changing ζ_1 in the stratified droplet model has a direct effect only on the molecules in the first layer, the consequences in the upper layers result from the coupling of the evolution equations. On the contrary, changing C_{fs} and D_{fs} plays directly on the two first layers because of the structure (and truncation) of the Lennard-Jones potential.

We report here results of simulations obtained in the complete wetting case at constant liquid−liquid interactions ($C_{ff} = D_{ff} = 1.0$) and for two sets of liquid/solid interactions ($C_{fs} = D_{fs} = 1.0$ and 5.0) corresponding to the "low" and "high friction" regimes, respectively.

It is known that MD simulations account well for the diffusive-like growth of the successive layers.[20] Therefore, only results on drop shape and molecules displacement will be reported.

Taking advantage of the cylindrical symmetry of the droplet shape, the atoms positions are fully determined by their distance R from the drop axis and their height z with respect to the substrate. To obtain information about the motion of the atoms inside the drop, let us consider a grid whose cells are unit squares in R and z variables. The atoms belonging to each cell of the grid are labeled and positions of the centers of mass of such sets are computed at a given time t. A few thousand time steps

(19) De Coninck, J.; Hoorelbeke, S.; Valignat, M. P.; Cazabat, A. M. *Phys. Rev. E* **1993**, *48*, 4549. De Coninck, J.; Fraysse, N.; Valignat, M. P.; Cazabat, A. M. *Langmuir* **1993**, *9*, 1906.

(20) De Coninck, J.; D'Ortona, U.; Koplik, J.; Banavar, J. R. *Phys. Rev. Lett.* **1995**, *74*, 928. D'Ortona, U.; De Coninck, J.; Koplik, J.; Banavar, J. R. *Phys. Rev. E* **1996**, *53*, 562. Cazabat, A. M.; Valignat, M. P.; Villette, S.; De Coninck, J.; Louche, F. *Langmuir* **1997**, *13*, 4754.

(21) Wagner, L. *Phys. Rev. E* **1995**, *51*, 499. Bekink, S.; Karaborni, S.; Verbist, G.; Esseling, K. *Phys. Rev. Lett.* **1996**, *76*, 3766.

(22) Lukkarinen, A.; Abraham, D. B.; Karttunen, M.; Kaski, K. *Phys. Rev. E* **1995**, *51*, 2199. Nieminen, J.; Abraham, D.; Karttunen, M.; Kaski, K. *Phys. Rev. Lett.* **1992**, *69*, 124.

(23) Blake, T. D.; Clarke, A.; De Coninck, J.; de Ruijter, M. J. *Langmuir* **1997**, *13*, 2164.

(24) Voué, M.; Valignat, M. P.; Oshanin, G.; Cazabat, A. M.; De Coninck, J. *Langmuir* **1998**. Manuscript to be published.

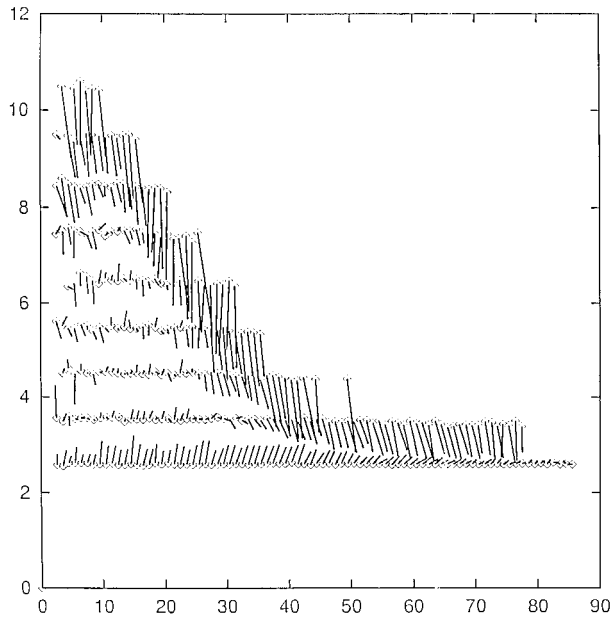

Figure 6. Molecules displacements calculated for the solid/liquid coupling parameters $C_{fs} = D_{fs} = 1.0$. They are computed at $t = 180 \times 10^3\,\Delta\tau$; the displacement of the atoms is evaluated over the next five 10^3 time steps.

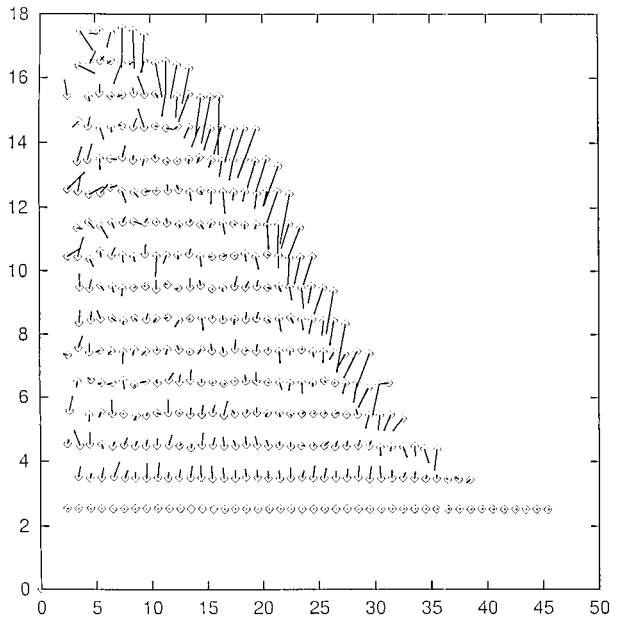

Figure 7. Molecular displacements calculated for the solid−liquid coupling parameters $C_{fs} = D_{fs} = 5.0$. They are computed at $t = 180 \times 10^3\,\Delta\tau$; the displacement of the atoms is evaluated over the next five 10^3 time steps.

later (i.e., at t+dt), the positions of these centers of mass are updated. Vectors joining these subsequent positions allow us to vizualize displacements inside the drop.

The method has the advantage to be simple and illustrative.[25] However, a quantitative interpretation of the results is not straighforward. The procedure does not exactly provide the Lagrangian velocity, because the thickness of a grid cell is the distance between layers (i.e., too small to ensure proper averaging in the vertical direction).

Profiles and "displacements" are represented on Figures 6 and 7 for the solid/liquid coupling parameters $C_{fs} = D_{fs} = 1.0$ and $C_{fs} = D_{fs} = 5.0$, respectively. They are computed at $t = 180\ 10^3\ \Delta\tau$ and the displacement of the atoms is evaluated over the next five 10^3 time steps.

In the "weak friction" regime ($C_{fs} = D_{fs} = 1.0$), only the two first layers are rapidly growing in front of the mesoscopic part of the drop. Important transfers of atoms from an upper layer to a lower one take place, even inside the drop. The profile is reminiscent of the ones in the stratified droplet model with $k \approx 1.2$, although the second layer is more developed, due to the LJ potentials used, as mentioned above.

As shown on Figure 7, in the nearly sticking regime ($C_{fs} = D_{fs} = 5.0$), the spreading of the drop proceeds very slowly and the radius of the first layer is only the half of the one measured at the same time in the "weak friction" regime. The drop shape is reminiscent of the one with $k \approx 0.2$ in the stratified droplet model, except for the second layer, for the same reason as before. The flow is considerably reduced, located close to the drop surface, and the atoms at the end of a layer tend to move more to the interior of the drop than to flow in the next lower layer.

In conclusion, these MD simulations satisfactorily capture the evolution of drop shape and dynamics, and agree well with the calculations on the stratified droplet model. Let us now present the experimental side of this study.

(25) De Coninck, J.; Voué, M. *Interface Sci.* **1997**, *5*, 141.

Experimental Observations

The questions discussed above were in fact raised by puzzling experimental observations. As expected, studies of mesoscopic precursor films of polymers below the 3-dimensional entanglement threshold showed that the "thickness dependent diffusion coefficient" was inversely proportional to the bulk viscosity η.[26−28] Less expectedly, this was found also for the few systems where we first investigated systematically the dependence of D_1 on chain length.[15]

The stratified droplet model has been developed for simple molecules, not polymers. But it suggests that the situation convenient to observe molecular effects is when a single layer spreads on the surface, which was not the case in the previous studies .[15] At given driving term, this can be obtained by reducing the friction, in which case only one layer develops.[18] If both driving term and friction change, we observed that the fastest film was actually a single layer.[29−30]

Therefore, a systematic study of the chain length dependence of D_1 was started again with specific reference to the observed drop shape.

As usual, drop profiles are recorded at successive times using a spatially resolved ellipsometer, the setup has been extensively described elsewhere[15,27−29]

The polymers are trimethyl-terminated poly(dimethylsiloxane)s (PDMS) below the three-dimensional entanglement threshold, and nonvolatile. The masses investigated range from 2 000 to 16 000. The lighter mass, with viscosity 0.02Po, cannot be fractionated and has a relatively large polydispersity index $I_p = 1.7$, but we checked that the mass distribution was monomodal, without lighter species. The larger masses are fractionated, with polydispersity indices between 1.06 and 1.20, and monomodal mass distributions. This range of mass is in the crossover between the asymptotic behavior below the entanglement threshold (i.e., $\eta \propto M$, and the asymptotic behavior above: $\eta \propto M^{3.4}$. In fact, the mass dependence of the viscosity in the range investigated is

(26) Novotny, V. J. *J. Chem. Phys.* **1990**, *92*, 3189. Marchon, B. Lecture at the Collège de France, September 1997, unpublished.

(27) Fraysse, N.; Ph.D. Thesis, University of Paris VI, 1991, unpublished.

(28) Valignat, M. P.; Fraysse, N.; Cazabat, A. M.; Heslot, F.; Levinson, P. *Thin Solid Films* **1993**, *234*, 475. Valignat, M. P.; Ph.D. Thesis, University of Paris XI, Orsay, 1994, unpublished.

(29) Heslot, F.; Cazabat, A. M.; Levinson, P.; Fraysse, N. *Phys. Rev. Lett.* **1990**, *65*, 599.

(30) Villette, S.; Ph.D. Thesis, University of Paris VI, 1996, unpublished.

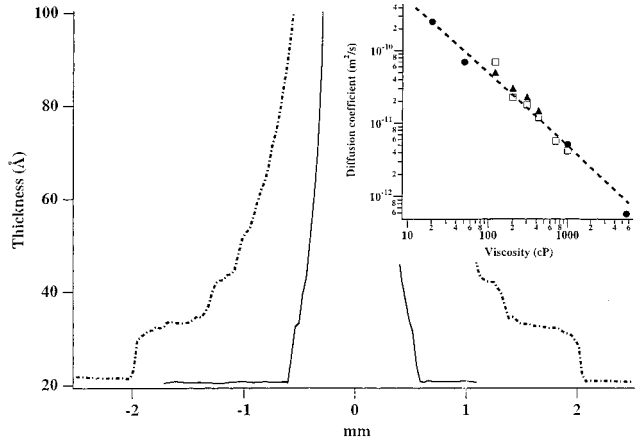

Figure 8. Ellipsometric profile of a PDMS microdroplet[26] after 3h30 (full line), and 70h30 (dotted). Molar mass $M_p = 16\,000$, viscosity 0.42Po, polydispersity index $I_p = 1.20$. The substrate is an oxidized silicon wafer bearing a noncompact grafted layer of trimethyl groups. Critical surface tension for alkanes ≈25.5 mNm^{-1}. Inset:[26,27,29] log−log plot of D_1 vs viscosity for various substrates. Squares: loose grafted layer. Dots: bare, uncleaned wafers. Triangles: cleaned wafers at RH ≈ 15%.

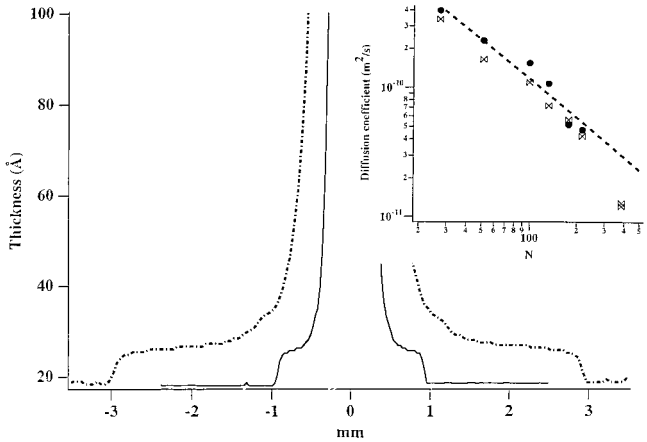

Figure 9. Ellipsometric profile of a PDMS microdroplet[26] after 3h30 (full line) and 48h (dotted). Molar mass $M_p = 16\,000$, viscosity 0.42Po, polydispersity index $I_p = 1.20$. The substrate is an oxidized silicon wafer bearing a compact grafted layer of trimethyl groups. Critical surface tension for alkanes ≈ 23 mNm^{-1}. Inset:[29] log−log plot of D_1 vs number of monomers for various substrates. Bowties: compact grafted layer. Dots: cleaned wafers at RH ≈ 40%.

very well fitted as $\eta \propto M^{1.7}$ (Petrarch Data). This allows us, hopefully, to make the distinction between the bulk parameter η and the molecular friction parameter ζ_1.

The substrates are oxidized silicon wafers. The type of drop profile observed depends on the surface preparation, and the previous discussions allow us to understand in which way (i) stepped profiles with several layers are observed on loose grafted trimethyl layers (wafers incubated with hexamethyldisilazane at room temperature with no specific care of hygrometric conditions[15,27,29]). Such a profile is given on Figure 8. Here, the driving term is weak and the friction moderate. Similar profiles, although with less steps, are obtained on bare wafers without cleaning,[26] or on bare, cleaned wafers at relative humidity RH less than 20%.[29−30] The former case is reminiscent of the wafer bearing a loose grafted layer, the latter corresponds to a different balance: both driving term and friction are higher, and the friction dominates.

(ii) Profiles with only one layer spreading out are obtained on compact grafted trimethyl layers (this is the case of Figure 9), Langmuir−Blodgett layers,[29] or bare, cleaned wafers at RH > 30%.[18] Here, the friction is low.

We repeated some experiments previously done on the first type of profiles, and recovered the trend $D_1 \propto \eta^{-1}$, these results are reported on the inset, Figure 8. Then we studied the second type of profiles. The results are reported on the inset, Figure 9. Except for the last point ($M = 28\,000$, above the threshold), the trend is now $D_1 \propto M^{-1} \propto N^{-1}$, where N is the number of monomers in the chain.

Note that, for high relative humidities, RH > 80%; the N-dependence of D_1 fades out. Ultimately, at RH ≈ 98%, D_1 becomes independent of N. This has been reported elsewhere[31] and interpreted as a change in the molecular friction process at very low friction.

Conclusion

We have performed a systematic study of the dynamics of growth of the first molecular layer of droplets of light, nonvolatile polymer oils, as a function of the chain length. The results depend on the drop profile, which in turn is controlled by a delicate balance between the two types of dissipation, in the bulk, where the relevant parameter is the viscosity η, or at the solid surface, where the relevant parameter is the friction coefficient ζ_1 between the first layer and the surface.

At large ζ_1, several steps develop in the drop profile and the measured diffusion coefficient D_1 of the first layer is inversely proportional to the bulk viscosity η. At low ζ_1, only one step develops and D_1 is inversely proportional to the friction coefficient ζ_1.

These observations are satisfactorily understood in terms of the stratified droplet model complemented by computer simulations. Moreover, we have used this opportunity to investigate the range of validity of the model, and to make clear in computer simulations what was specific of the physical process and what was due to the truncation of the interaction potential used. Therefore, a deeper understanding of the physical processes and of the models themselves has been achieved.

Acknowledgment. This work has been partially supported by the HCM Network Grant CHRX-CT9-0448, and by the 97.013 Tournesol exchange program.

LA9805600

(31) Valignat, M. P.; Oshanin, G.; Villette, S.; Cazabat, A. M.; Moreau, M. *Phys. Rev. Lett.* **1998**, *80*, 5377.